ACS Photonics

Article

pubs.acs.org/journal/apchd5

Efficient Pump Photon Recycling via Gain-Assisted Waveguiding Energy Transfer

Roy Aad,[†] Christophe Couteau,*[,†] Sylvain Blaize,[†] Evelyne Chastaing,[‡] Françoise Soyer,[‡] Laurent Divay,[‡] Christophe Galindo,[‡] Pierre Le Barny,[‡] Vincent Sallet,[§] Corinne Sartel,[§] Alain Lusson,[§] Pierre Galtier,[§] Licinio Rocha,[∥] Vesna Simic,[∥] and Gilles Lérondel*[,†]

[†]Laboratoire de Nanotechnologie et d'Instrumentation Optique (LNIO), Institut Charles Delaunay, CNRS UMR 6279, Université de Technologie de Troyes (UTT), 12 rue Marie Curie, 10010, Troyes France

[‡]Laboratoire de Chimie des Matériaux Organiques, THALES Research and Technology, Campus Polytechnique, 1 avenue Augustin Fresnel, 91767 Palaiseau, France

[§]Groupe d'Etude de la Matière Condensée (GEMAC), CNRS-UVSQ, 45 avenue des Etats-Unis, 78035 Versailles, France

[∥]CEA, LIST, Laboratoire Capteurs et Architectures Electroniques, 91191 Gif-sur-Yvette, France

S *Supporting Information*

ABSTRACT: We propose a new concept for enhancing the fluorescence of ultrathin nanolayers. In this article, we address the issue of efficient absorption of polymer thin films with nanometer characteristics. For many applications, such as sensing, but also for lighting or photovoltaics, devices require the use of nanometer-sized films of a specific polymer or a luminescent nanolayer in general. Usually, most studies are geared toward enhancing the emission of such luminescent films via Bragg mirror-type cavities, for instance, but little attention is paid for optimizing the absorption of the thin films. We show the principle of gain-assisted waveguiding energy transfer (G-WET) by inserting a gain-active layer between an active nanometer-scale layer (a luminescent polymer in our case) and the passive substrate. Efficient absorption via "recycling" of the pumping photons is ensured by the waveguiding effect due to this high-index active layer. To demonstrate the G-WET effect, two kinds of samples were studied. They consist of extremely thin (~10 nm) polymer nanolayers spin-coated either on quartz, referred as the passive case, or on a ZnO active thin film (~170 nm, acting as a gain medium) grown on sapphire, referred as the active case. Samples were characterized by room-temperature photoluminescence (PL) spectroscopy under various pumping intensities. Compared to the quartz substrate, the ZnO thin film induces a remarkable enhancement of a factor ~8 on the fluorescence of the polymer nanolayer. Observations show that, for the passive quartz substrate case, the PL of the spin-coated polymer rapidly saturates, defining a luminescence limit; whereas, with the active ZnO layer, the polymer presents a nonlinear PL intensity surpassing the saturation level. This new photonic system revealed that the polymer luminescence enhancement is the result of both an efficient energy transfer and a geometrical effect ensured by an evanescent coupling of the waveguided ZnO stimulated emission. Although our work discusses the specific organic−inorganic case of fluorescent polymer and ZnO, the G-WET concept can be generalized to any hybrid layered sample verifying the necessary energy transfer conditions discussed in this article, thus, demonstrating that this is of a special interest for efficient absorption and efficient recycling of the excitation photons for any nanometer scale fluorescent layer.

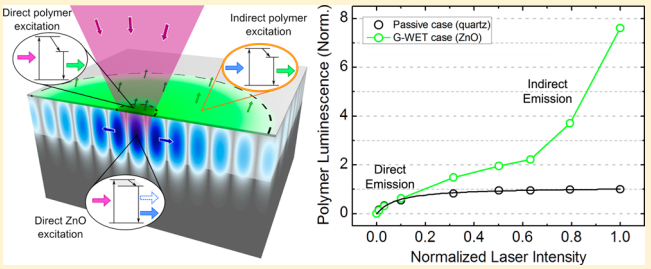

KEYWORDS: *absorption, emission, ultrathin nanolayer, energy transfer, optical gain, waveguide, fluorescent polymer, zinc oxide*

For many applications such as photovoltaic, lighting, lasing, or sensing, efficient absorption and efficient emission of luminescent nanometer-scale layers is desirable. Whereas most of the studies are dedicated to optimize the emission of such layers, very few studies tackle the issue of optimizing the absorption of these fluorescent nanolayers. The best known example is probably a semiconductor quantum well embedded between two highly reflecting Bragg mirrors. In this case, many quantum wells can be embedded within such a structure and the mirrors provide the feedback and the directionality of the lasing emission in VCSEL for instance.[1] In photovoltaics, efficient absorption is of primary importance. Nowadays, one line of research for optimizing solar cells is to engineer thin efficient absorbers using plasmonics and metamaterials.[2] Near-perfect absorption was also achieved using graphene[2] and can have applications in communications too.[3] The idea is to reduce the absorption layer thickness from few hundreds μm to submicrometer thickness of silicon or other type of hybrid semiconductor-metal material. For sensing applications, con-

Received: November 11, 2013
Published: February 10, 2014

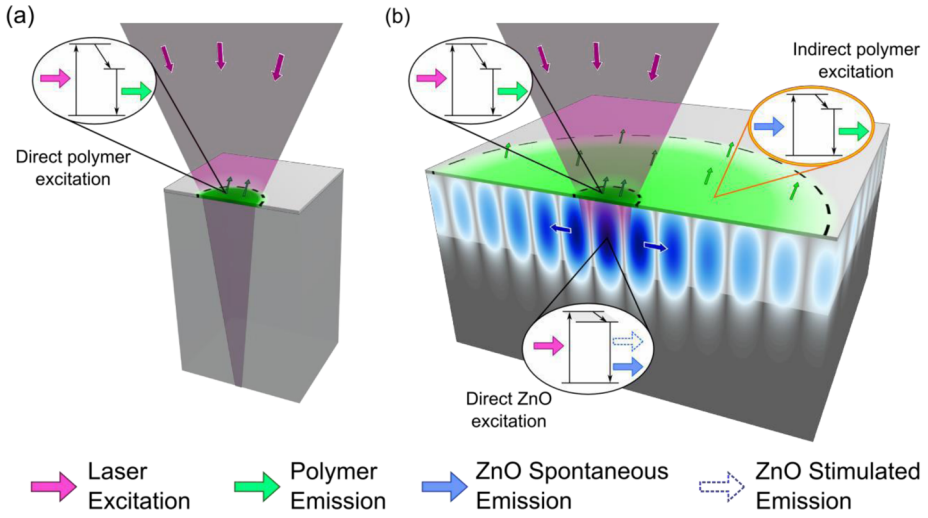

Figure 1. Art picture of the gain-assisted waveguiding energy transfer (G-WET) process for ultrathin film optimized excitation as illustrated for a (polymer) luminescent thin film and an active (ZnO) layer. (a) Case of the passive substrate. A fluorescent polymer layer (light gray) spin-coated on quartz (transparent light blue) is excited by a focused laser beam (transparent violet). The laser spot defines the luminescent polymer area (highlighted in green). The callout bubble represents a brief sketch of the polymer photoluminescence process. (b) Case of the active layer. The fluorescent polymer layer is now spin-coated on ZnO (lighter gray) grown on sapphire (dark gray). A laser beam is again directed toward the structure and excites an equivalent polymer area (limited by the small dashed circle). The laser beam continues toward the ZnO thin film where it is completely absorbed. The ZnO thin film luminesces and preferably couples its emission into a guided mode, represented by the blue guided mode profile. The ZnO guided mode spreads throughout the thin film and repeatedly excites the polymer. Thus, the ZnO excited polymer presents a much larger luminescent area (limited by the large dashed circle). In a similar fashion, the callout bubbles represent the laser (direct) polymer and ZnO excitation and the ZnO (indirect) polymer excitation processes. The dashed blue arrow pictures the stimulated emission.

sidering the thicknesses involved, the cavity configuration is not possible. Fluorescence quenching polymers have proven to be potentially interesting materials for achieving highly selective and extremely sensitive detection of gas molecules in atmosphere.[4,5] But the polymer layers are required to be extremely thin (<20 nm) in order to exhibit fast response times and low detection thresholds.[6] The reduction of the polymer thickness is accompanied by a decrease in the absorption as well as a decrease in the quantity of fluorescent polymer chains, which are both responsible for a strong weakening of the fluorescent intensity of the polymer layer. Thus, the recent studies on sensing have focused on the fluorescence enhancement of ultrathin polymer nanolayers.

The subject of enhancing the fluorescence of emissive nanometer-size luminescent material was recently tackled by Rose et al. for sensing applications with polymers.[7] In this work, the authors addressed the fluorescence enhancement issue through a lasing action in the organic polymer layer which induced a superlinear increase in the polymer fluorescence and eventually led to a gain in sensitivity. Another related work by Liu et al. showed that waveguiding within nanowires of different lengths could select the lasing mode of the nanowire.[8] This is done by intrinsic self-absorption at the Urbach tail states of the light emitted from a CdS nanowire. This is another example of using waveguiding and reabsorption of the pump photons in order to achieve mode selection. However, no existing study has yet discussed on enhancing the weak absorption of the layer rather than optimizing its luminescence. The issue of very low absorptions remains one of the main unresolved problems limiting the fluorescence of nanometer size layers or nanostructures such as nanowires. In this article, we propose, and later on demonstrate, a new general photonic concept of gain assisted waveguiding energy transfer (G-WET) for efficient nanothin film luminescence excitation.

Figure 1 presents two 3D illustrations that clarify the luminescence excitation issue and the proposed G-WET concept. Figure 1a represents the so-called standard case of a nanometer thick fluorescent layer (in our case a polymer) on a passive (nonemitting) quartz substrate. According to Beer–Lambert's law, ultrathin (<20 nm) polymer layers absorb an extremely small percentage of the pumping intensity. As an example for the polymer material studied in this article, with an absorption coefficient of 7.10^{-4} nm^{-1} at 337 nm, less than 1.5% of the pumping intensity is absorbed. For devices fabricated with optically passive supports such as quartz, as illustrated in Figure 1a, only a very small amount of the laser excitation (in violet) is used to excite the polymer emission (in green) and the rest is "wasted" without benefit by going through the substrate. Replacing the standard quartz plate with an active layer made of a high refractive index material with gain is an effective solution to the weak polymer luminescence excitation. This active layer is the core of the G-WET phenomenon proposed here and illustrated in Figure 1b. In addition to the direct excitation by the laser (in violet) leading to an excited area defined by the laser spot size (dashed circle), the presence of the active layer that can absorb and reemit photons in a guided configuration leads to a larger polymer emitting surface (larger dashed circle). Let us now describe in more detail the different steps of the G-WET process. In order to have an optimized energy transfer, the active layer needs to be thick enough to absorb all the incident laser intensity as illustrated on the figure by the purple gradient. By the same token, to obtain an efficient transfer, the active layer luminescence needs to be as high as possible and to lie in the polymer absorption range. Nonetheless, the energy transfer (ET) process is most efficient if it is provided by the evanescent tail of the waveguided modes within the active layer in order to prevent the emitted photons to escape toward the substrate. The idea is the same when one wants to pump efficiently nanostructures such as nanowires to

dx.doi.org/10.1021/ph4001179 | ACS Photonics 2014, 1, 246–253

achieve lasing emission. Figure 1b depicts the waveguiding effect in the active layer with the intensity profile of a guided mode propagating inside the active layer. With G-WET, waveguiding is present if the active layer is made of a high refractive index material. This essential element insures that guided modes stay strongly confined inside the active layer (ZnO in our case), subsequently realizing a great number of round trips within the layer thickness. In this configuration, the guided mode will repeatedly excite the polymer layer through the tail of its evanescent wave, which constitutes the most adequate configuration for an efficient ET process.[9] The guided modes spreading throughout the slab can excite polymer chains lying outside the laser spot, thus, extending the polymer luminescent surface and inducing a "geometrical" effect. The active layer thickness therefore should not exceed the limits of a single-mode waveguide in order to provide the best waveguiding configuration. The active layer luminescence must particularly couple to the fundamental mode which presents the highest effective index[10] and, in effect, the weakest losses. Finally, we must stress that another factor is important in our system. Figure 1b represents the fact that the active layer is a gain medium which can then show stimulated emission (dashed blue arrow). This gain factor constitutes the final piece of the proposed G-WET concept as the stimulated emission amplifies the luminescence and therefore improves the quantum yield of the active layer. Equally, this amplified emission improves the propagation of the guided mode, as the attenuation inside the active layer is reduced. In the following, we present an experimental study which demonstrates the previously discussed G-WET concept by considering the specific case of ultrathin poly[dimethyl-*co*-methyl-(1,1,1-trifluoro-2-(trifluoromethyl)-2-oxy-pent-4-yl)-*co*-(methyl-(4-pentyloxy-(*N*-(2,5-di-*tert*-butylphenyl))-1,8-naphthalimide)]-siloxane[11−14] (cf. Supporting Information) called the fluorescent polymer layer later on. The fluorescent polymer layer is spin-coated on a ZnO film grown on a sapphire substrate (equivalent to some extent to the standard quartz substrate by its optical properties).

This copolymer was designed to detect nitroaromatic compounds, more specifically, 2,4-dinitrotoluene and 1,3-dinitrobenzene[11] (chemical compound signatures found in military grade TNT), by fluorescence quenching of the fluorescent chromophores located in its side chains. However, in this paper, this fluorescent polymer was used because it exhibits an absorption in the 375 nm range which matches with the peak emission of ZnO. The fluorescent polymer also exhibits an important Stokes shift (emission peak at 468 nm) which here allows to clearly separate the two emission contributions of the fluorescent polymer (ultrathin film) and the ZnO (active layer).

ZnO was chosen as an adequate active support according to its optical properties. As subsequently detailed, ZnO exhibits a UV emission[15−19] that is particularly well-adapted for exciting the studied polymer layer. Compared to sapphire (n = 1.8 at 375 nm) and the polymer (n = 1.56 at 375 nm), ZnO has a high refractive index[20,21] (n = 2.57 at 375 nm) and thus forms the waveguided layer mentioned earlier. Moreover, stimulated emission and gain are reported under high pumping intensities.[16−19,22−29]

Two sets of samples were prepared for this study (Table 1). The first set (**S0**) consisted of a polymer nanolayer on quartz substrate (used as a reference), while the second set (**S1**) was formed by a polymer nanolayer on ZnO film itself grown on sapphire substrate. To fabricate the samples, a polymer solution

Table 1. List of the Studied Samples

	sample name	
	S0	**S1**
description	polymer nanolayer spin-coated on quartz plates	polymer nanolayer spin-coated on ZnO thin film (∼170 nm; cf. Supporting Information)

(1.6 mg·mL^{-1} in methylethyl ketone) was spin-coated on quartz plates and on ZnO thin films with a spin rate of 3200 rpm for 30 s. Samples were then stored under vacuum at room temperature to remove the solvent. The spin-coated polymer formed an 8−10 nm thick nanolayer. ZnO thin films used to prepare the **S1** samples were 170 nm thick and were grown on R-sapphire by metal−organic chemical vapor deposition (MOCVD; cf. Supporting Information). Samples were characterized using room-temperature photoluminescence (PL) spectroscopy in order to study the impact of the ZnO thin film on the polymer fluorescence. PL was conducted using a pulsed nitrogen laser (λ = 337.1 nm, 4 ns pulse duration) operating at a repetition rate of 10 Hz. The laser beam was focused by a lens onto an 1 mm diameter spot with an average power of 40 μW. Luminescence was collected using an objective lens with a 0.13 numerical aperture focused onto a large core (400 μm diameter) optical fiber connected to a 50 cm focal length spectrometer equipped with a CCD Peltier-cooled camera.

To investigate the influence of the ZnO waveguide, the polymer fluorescence intensity was measured as a function of power using neutral density (ND) filters. Figure 2 shows the

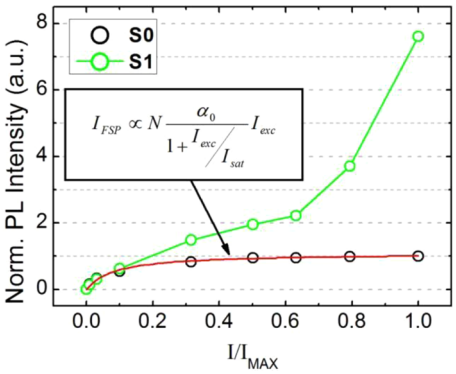

Figure 2. Comparison between the photoluminescence of the fluorescent polymer film coated on quartz, **S0** sample (black circles) and on the ZnO layer, **S1** sample (green circles) as a function of the normalized pumping intensity (I/I_{max}). The plotted PL intensity values are taken at λ_{em}^{max} (∼468 nm) and normalized by the maximum PL intensity recorded for the **S0** sample.

evolution of the PL intensity as a function of the normalized pumping intensity (I/I_{max}), for both **S0** and **S1** samples at 468 nm, which corresponds to the λ_{em}^{max} of the polymer fluorescence peak. From hereafter, unless otherwise indicated, all the presented spectra and PL intensities are normalized by the maximum λ_{em}^{max} value presented by **S0**. Figure 2 reveals a distinct difference in the polymer fluorescence dependence between the two samples.

For **S0**, the polymer fluorescence (black circles) rapidly saturated and reached a maximum intensity limit as the pumping intensity was increased. The maximum fluorescence is related to the polymer nanolayer thickness and, hence, the

dx.doi.org/10.1021/ph4001179 | ACS Photonics 2014, 1, 246−253

number of fluorescent naphthalimide moieties (N) present in the layer. Moreover, the polymer fluorescence behavior can be well described by an absorption saturation[30] that subsequently leads to the fluorescence saturation.[31] The rapid absorption saturation can be attributed to the ultrathin layer thickness (i.e., very small N). Considering a linear fluorescence dependency, the calculated curve fit (red line) can be expressed in the following manner,

$$I_{FSP} \propto -N \cdot dI/dx = N \cdot \alpha \cdot I_{exc} = N \frac{\alpha_0}{1 + (I_{exc}/I_{sat})} I_{exc} \quad (1)$$

where α_0 is the polymer absorption coefficient for moderate excitation, N is the number of fluorescent naphthtalimide moieties present and I_{FSP}, I_{exc}, and I_{sat} are, respectively, the fluorescent polymer, pumping, and saturation intensities.

On the other hand, for **S1**, the polymer fluorescence (green line) did not saturate even at a high pumping intensity. At low pumping intensities ($I/I_{max} \leq 0.1$), **S1** presented similar polymer fluorescence levels as **S0**. However, as pumping intensity was further increased, **S1** polymer fluorescence exhibited a superlinear dependency and rapidly exceeded the **S0** values. The fluorescence increase surpassed the saturation limits eventually reaching an up to ~8-fold increase at the maximum pumping intensity. Because the polymer fluorescence presented no saturation tendency, that leaves room for further enhancement with improved experimental conditions. Figure 2 shows the important influence of the ZnO slab on the polymer fluorescence.

In order to understand the origin of the **S1** superlinear increase, it is essential to first verify that this behavior is not an artifact resulting from a spectral overlap between the polymer and a ZnO defect emission. It is therefore important to separately characterize the PL spectrum of the ZnO slab used to fabricate **S1** and, thus, verify if the PL intensity measured at 468 nm (Figure 2) is solely due to the polymer fluorescence. For this purpose, a portion of the **S1** sample was not coated by the polymer in order to measure the ZnO PL. Figure 3 displays the ZnO emission spectrum (dashed black line) along with the polymer emission (black line) and absorption (blue line) spectra. All the spectra in Figure 3 are normalized by their respective maximum. The collected PL spectrum does not show the presence of ZnO related defect emission. Instead,

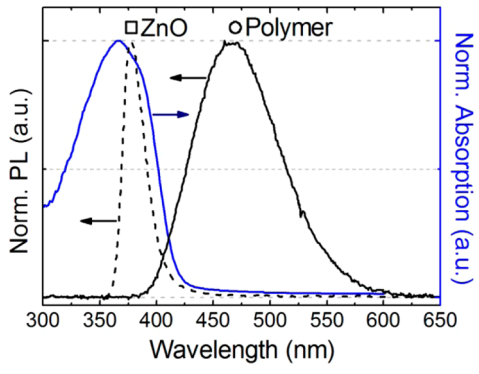

Figure 3. Fluorescence (straight black line) and absorption (straight blue line) spectra of the fluorescent polymer, along with the luminescence spectrum of the ZnO layer (dashed black line). The square and circle, respectively, indicate the ZnO and fluorescent polymer emissions. All presented spectra are normalized to 1, while the arrows mark the corresponding y-axis.

ZnO manifests a single emission peak in the UV (λ_{em}^{max} = 375 nm) that is widely separated from the polymer fluorescence (λ_{em}^{max} = 468 nm). The wide spectral separation is a favorable aspect for this study, as it prevents unwanted spectral overlapping that can contribute to the collected PL intensity at 468 nm and, therefore, complicate the quantitative analysis of the polymer fluorescence. The emission spectra shown in Figure 3 clearly indicate that the behavior observed for **S1** (as seen in Figure 2) is indeed due to a polymer fluorescence enhancement.

In the meantime, Figure 3 displays another essential feature of the polymer and ZnO layers and an indispensable condition of the proposed concept as it reveals a perfect spectral overlap between the polymer absorption spectrum and the ZnO luminescence spectrum. This spectral "matching" is one of the primary reasons for the choice of ZnO as it insures an efficient polymer excitation (i.e., energy transfer) by the ZnO luminescence. Figure 3 therefore points out to a probable radiative energy transfer that could explain the superlinear polymer fluorescence of **S1**.

In addition to the radiative energy transfer, one can speculate the nonlinear polymer enhancement (seen in Figure 2) to be the result of a stimulated polymer emission, occurring at high pumping intensities. However, it should be clear that this is not the case for the studied polymer. Indeed, if the nonlinear polymer enhancement were due to stimulated emission, then it should have been also observed on **S0**. Furthermore, the occurrence of a stimulated emission can be utterly revoked when looking at the spectral features of the polymer fluorescence. Figure 4 presents the PL spectra of **S0** (a) and **S1** (b), corresponding to the polymer fluorescence intensities shown in Figure 2. As it is seen in Figure 4a and 4b, the polymer fluorescence presents a constant λ_{em}^{max} at 468 nm and hardly any change in the full width at half-maximum (fwhm); which ranged between 86 and 90 nm, for the various pumping intensities. However, stimulated emission is normally characterized by a λ_{max} shift and strong narrowing of the fwhm in the luminescence peak. The present polymer fluorescence features exclude the presence of polymer stimulated emission. We would like to point out that nonradiative energy transfer (NRET) processes can also lead to a nonlinear enhancement of the polymer fluorescence. Indeed, NRET processes can occur between organic–inorganic materials.[32,33] However, these processes are extremely sensitive to donor densities and donor–acceptor coupling and distances. Therefore, NRET processes are more observed between high quality interfaces and for materials presenting a strong exciton confinement at the interface, such as ZnO/ZnMgO quantum wells.[33−35] This is not the case here, the studied configuration consists of a polymer layer that is spin-coated on a ZnO (170 nm) thin film. Thus, the studied configuration does not present the high quality interface and the strong exciton confinement that are needed to obtain a good NRET efficiency (for a quantitative analysis of the exciton confinement effect in similar system see ref 36). PL measurements realized on a similar polymer layer that was spin-coated on a ZnO thin film but of lower optical quality (i.e., exhibiting no gain or stimulated emission) show no effect on the polymer emission. More precisely, a study of the evolution of the fluorescence intensity as a function of the pumping intensity of the polymer layer deposited on lower optical quality ZnO thin film reveals a similar PL dependency (peak and saturation intensity) to that exhibited by **S0** in Figure 2 (results not shown). The latter observation proves that

dx.doi.org/10.1021/ph4001179 | ACS Photonics 2014, 1, 246−253

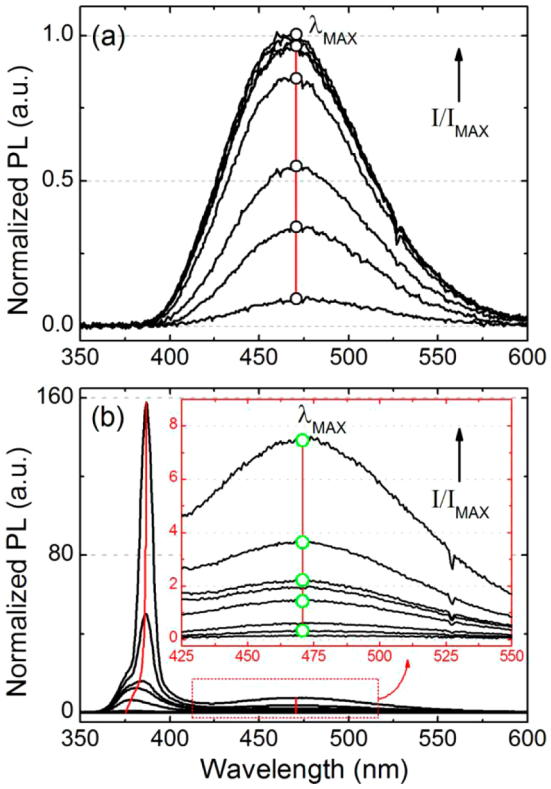

Figure 4. Luminescence spectra of the polymer fluorescent film coated on quartz, **S0** sample (a), and on the ZnO layer, **S1** sample (b), corresponding to the PL dependency in Figure 2. In analogy, all PL spectra are normalized by the maximum PL intensity recorded for the **S0** sample. The red lines show the spectral shift of λ_{em}^{max} for the various polymer and ZnO luminescence peaks. The presented black (a) and green (b) circles, respectively, indicate the plotted values for the **S0** and **S1** samples in Figure 2. The arrow in (a) and (b) represent the direction of the ascending I/I_{max}. The inset in (b) shows a zoom of the polymer fluorescence.

NRET processes are negligible in the studied polymer/ZnO system. However, a study of the PL dynamics, such as in refs 32 and 33, is of need in order to be more quantitative on the contribution of NRET processes in the studied system. Such a study is beyond the scope of the paper. As shown later in the article, the nonlinear polymer enhancement (cf. Figure 2) is indeed the result of an efficient radiative energy transfer due to the absorption by the polymer thin film of the ZnO waveguided spontaneous amplified emission, that is, evanescent optical coupling.

As previously mentioned, the energy transfer is achieved through the absorption of the ZnO luminescence by the polymer. Hence, investigating the ZnO luminescence can uphold results that further confirm the transfer. Additionally to the polymer fluorescence peak, the **S1** spectra presented in Figure 4b show a ZnO related luminescence peak. Contrary to the polymer, the ZnO luminescence exhibited a remarkable change in its spectral features with increasing pumping intensity (indicated by the arrow direction). Under moderate pumping intensities, the ZnO spectra presented a spontaneous excitonic emission peak at $\lambda_{em}^{max} \sim 376$ nm with fwhm ~ 23 nm. However, as the pumping intensity was increased, a new emission peak appeared at the lower energy shoulder ($\lambda_{em}^{max} \sim 386$ nm) of the previous peak, which presented a narrowing of the line width (fwhm ~ 9 nm) as well as a behavior with the power excitation suggesting stimulated emission.

By plotting λ_{em}^{max} in a log–log graph, the power orders of the ZnO luminescence dependency can be determined. Figure 5

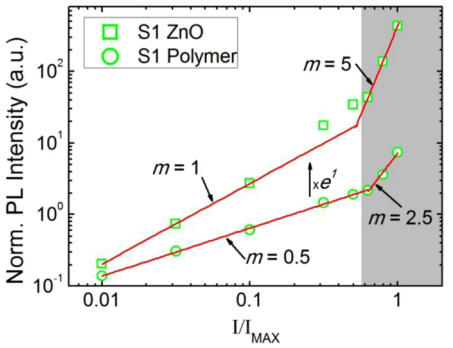

Figure 5. Log–log graph of the PL dependency of the **S1** sample with the polymer (green circles) and ZnO (green squares) luminescences as a function of I/I_{max}. The red lines show the linear fits. Each of the plotted PL intensity values are taken at the corresponding λ_{em}^{max} (shown in Figure 4b). The ZnO dependency is multiplied by e^1 to have a better separation from the fluorescent polymer dependency.

presents a log–log plot of the ZnO PL intensity for **S1** (green squares) taken at λ_{em}^{max} (marked by the red line in Figure 4b) for different power excitations. Figure 5 reveals a linear dependency for the first ZnO peak ($\lambda_{em}^{max} \sim 376$ nm), collected at low pumping intensities. On the other hand, the second ZnO peak ($\lambda_{em}^{max} \sim 386$ nm), appearing at high pumping intensities, manifested a fifth order superlinear increase. The first and second ZnO peaks can be therefore attributed to ZnO excitonic emission (E_{ex}-line) and electron–hole plasma stimulated emission (N-line),[16,18] respectively.

Furthermore, the polymer fluorescence dependency of **S1** (shown in Figure 2) is also plotted in Figure 5 (green circles). Comparing the polymer and ZnO luminescence intensities, Figure 5 shows that a superlinear increase is simultaneously exhibited in both cases. Under moderate pumping intensities, the polymer presented a sublinear fluorescence dependency with a ~0.5 order ($I_{FSP} = I_{exc}^{0.5}$) typical from a saturation-type power dependence, cf. eq [1]. On the other hand, as the ZnO layer passed the stimulated emission threshold, the polymer exhibited a superlinear fluorescence dependency of ~2.5. The sublinear fluorescence dependency suggests that the superlinear fluorescence dependency of the polymer is due to a fifth order excitation ($I_{FSP} \propto I_{exc}^{2.5} = (I_{exc}^{5})^{0.5}$), which is precisely the one found for the ZnO active layer case. We can conclude clearly that the superlinear dependencies point out to a strong relation between the polymer fluorescence and the N-line, thus, proving without any doubt the occurrence of an efficient radiative energy transfer. However, the obtained results shown so far neither clarifies the origins of the strong interdependence of the polymer fluorescence to the N-line nor explains how the **S1** polymer fluorescence surpasses the saturation limit (cf. Figure 2). For that, as suggested previously, we need to take the waveguiding effect from the active layer into account. Throughout the study, both **S0** and **S1** samples were excited by the same laser spot (Ø 1 mm). The laser spot thus defines similar excited volumes of the polymer layer on both samples. Taking this into consideration, both samples should saturate at equal polymer fluorescence intensities. Nonetheless, the polymer fluorescence levels of **S1** appear not to be defined

dx.doi.org/10.1021/ph4001179 | ACS Photonics 2014, 1, 246–253

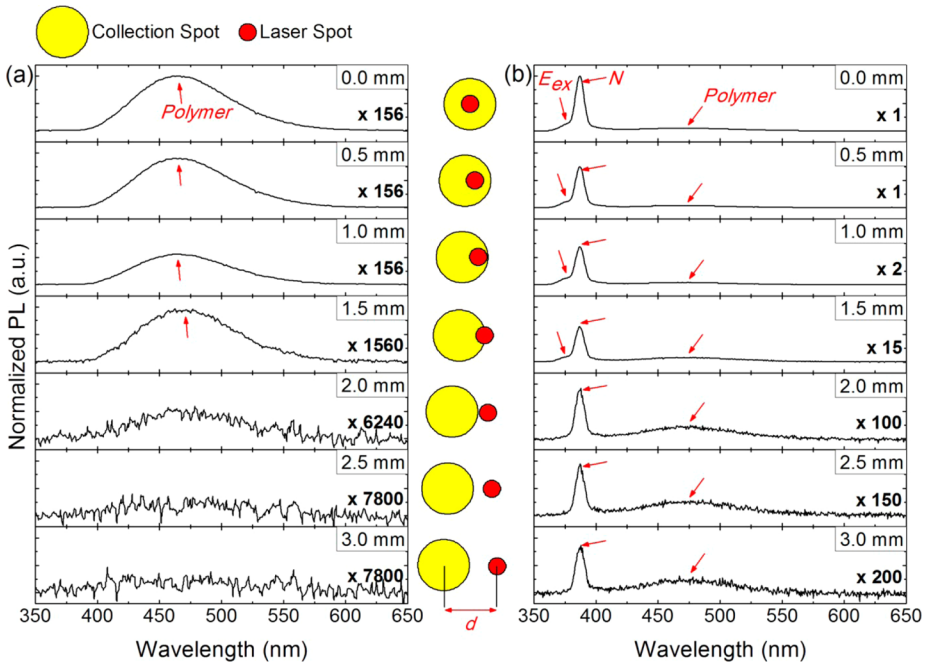

Figure 6. Evolution of the PL spectra for the polymer fluorescent film coated on quartz, **S0** sample (a), and on the ZnO layer, **S1** sample (b), as a function of the distance (d) separating the center laser spot and the axis of the collection objective. The PL spectra are all plotted on the same y-axis scale and normalized by the PL intensity recorded at the λ_{em}^{max} of the N-line for d = 0 mm. The inset between the two figures presents a sketch of the evolution of d.

by the pumped laser volume. This observation suggests the existence of an additionally excited volume of the polymer due to a geometrical (i.e., waveguiding) effect.

To confirm the presence of a geometrical effect, the collection lens axis was gradually misaligned in the horizontal direction, in order to vary the distance d between the lens axis and the center of the laser spot (inset Figure 6). The PL measurements were conducted at the highest pumping intensity (i.e., no neutral density filters were used) in order to provide the best conditions for obtaining ZnO stimulated emission. Figure 6 shows the evolution of the **S0** (a) and **S1** (b) spectra with increasing d (from top to down). Regarding **S0**, Figure 6a exhibits a polymer fluorescence that gradually decreases as d increases. Eventually, the fluorescence almost totally diminishes for $d \geq 2$ mm. At d = 2 mm, the collection (Ø ∼ 3 mm) is tangent to the laser spot (Ø ∼ 1 mm) on the outer side of the spot. Hence, for **S0**, Figure 6a clearly shows that the excited polymer area is definitely outside of the laser spot. On the other hand, regarding **S1**, Figure 6b manifested a polymer and ZnO luminescence spectra, which also decreased with increasing d but, in this case, the PL spectra collected outside the laser spot ($d \geq 2$ mm) still displayed a persisting luminescence. Compared with **S0**, **S1** clearly presents a much wider luminescent area. Thus, Figure 6b reveals the existence of a geometrical effect that clarifies the origins of the **S1** polymer enhancement. By waveguiding, the excitation area of the polymer simply increases further than just under the laser spot, hence, exciting more polymer chains.

Furthermore, the ultrathin polymer layer does not support any guided modes, which means that outside the laser spot ($d \geq 2$ mm), the observed polymer fluorescence is neither guided in the **S1** structure nor excited by the laser. Clearly, the observed polymer fluorescence is excited by the evanescent tail of the ZnO luminescence guided through the slab. On the other hand, the ZnO layer (170 nm) does constitute an efficient slab waveguide,[10,22] and as a consequence, the ZnO luminescence is mostly coupled into guided modes.[37] Therefore, it is logical to assume that the ZnO luminescence (N-line), collected for $d \geq 2$ mm, results from guided modes. This assumption is further confirmed by the evolution of the ZnO luminescence features observed in Figure 6b. For $d < 2$ mm, while the collection and laser spots still overlap, Figure 6b presents a double-peaked ZnO luminescence. The ZnO luminescence shape results from the overlap of the E_{ex}-line ($\lambda_{em}^{max} \sim 376$ nm) and N-line ($\lambda_{em}^{max} \sim 386$ nm). However, as soon as the collection spot is no longer in coincidence with the laser spot ($d \geq 2$ mm), Figure 6b shows that only the N-line remains. Evidently, the E_{ex}-line is only collected from inside the laser excited surface, while the N-line is collected from both inside and outside the laser excited surface. This can be explained easily by the fact that ZnO thin films manifest a strong and abrupt change in the attenuation coefficient k at the bandgap (∼376 nm).[20,21] Consequently, a small red-shift in the wavelength, from 376 nm (E_{ex}-line) to 386 nm (N-line), induces a colossal decrease in k from 0.3 to 0.05,[20] respectively. The E_{ex}-line is therefore strongly attenuated inside the ZnO slab and is not seen outside the laser spot area. This effect of reabsorption is well-known in waveguiding in long semiconductor nanowires and was observed many times.[8,38] Moreover, at 386 nm, the ZnO slab is single mode,[10] and thus, the N-line is coupled into the fundamental mode, which leads to its efficient waveguiding throughout the slab. As a consequence, only the N-line is observable from outside the laser spot. Figure 6b, thus, demonstrates that the N-line is solely contributing to the "geometrical" effect discussed previously.

To conclude, we presented in this article a new concept to enhance the absorption and therefore the luminescence of ultrathin fluorescent nanolayers for optical applications requiring very thin active layers such as sensing or lasing.

dx.doi.org/10.1021/ph4001179 | ACS Photonics 2014, 1, 246−253

Using a gain assisted waveguiding energy transfer (G-WET), we showed that a factor of 8 can be gained for the polymer nanolayer luminescence with our system and, thus, potentially decrease by the same amount the sensing threshold of detectors making use of this effect for instance. We specifically considered the case of fluorescent polymer−ZnO hybrid structures, which consisted of a simple multilayer geometry as planar geometry is easy to fabricate and has the advantage of being homogeneous and rigid. Yet, the fluorescent polymer−ZnO system presents an enhanced luminescence compared to typical samples of polymer on quartz. The experimental investigation revealed the fluorescence enhancement to be the result of an energy transfer and a geometric effect. The geometric effect is shown to be the consequence of guided ZnO stimulated emission as the guided emission propagates along the ZnO thin film and excites a wider polymer nanolayer area. We showed a way to "recycle" laser pumping photons that are usually wasted in the passive substrate. The obtained results validate the proposed concept and show the necessity of using an active waveguiding media as support. In general, we think that the G-WET method allows one to lower the pumping level of the excitation photons, provided that an active layer with particular properties (right thickness, matching absorption, waveguiding, gain medium) is inserted between the fluorescent nanolayer and the passive substrate. In an ultimate approach, the G-WET concept can eventually be combined with nanostructured active layers such as 2D photonic crystals or self-formed cavities that can present reduced lasing threshold due to dielectric confinement, as recently demonstrated in ref 39. This concept goes beyond the presented structure of fluorescent polymer and ZnO and can be used for other hybrid structures.

■ ASSOCIATED CONTENT

Ⓢ Supporting Information

Information concerning the synthesis of the fluorescent polymer and the growth of the ZnO thin film. This material is available free of charge via the Internet at http://pubs.acs.org.

■ AUTHOR INFORMATION

Corresponding Author

*E-mail: couteau@utt.fr; lerondel@utt.fr.

Notes

The authors declare no competing financial interest.

■ ACKNOWLEDGMENTS

This work was supported by the ANR Project ULTRAFLU and the CPER Project MATISSE. One of the authors, R.A., would like to thank the Champagne-Ardenne regional council for the Ph.D. support. The authors would also like to thank Loïc LE CUNFF for his help in preparing the figures.

■ REFERENCES

(1) Peters, F.; Peters, M.; Young, D.; Thibeault, B.; Corzine, S.; Coldren, L. High-Power Vertical-Cavity Surface-Emitting Laser. *Elec. Lett.* **1993**, *29*, 200−201.

(2) Atwater, H. A.; Polman, A. Plasmonics for Improved Photovoltaic Devices. *Nat. Mater.* **2010**, *9*, 205−213.

(3) Zhang, J.; MacDonald, K. F.; Zheludev, N. I. Controlling Light-with-Light without Nonlinearity. *Light Sci. Appl.* **2012**, *1*, e18.

(4) Melinte, V.; Buruiana, T.; Tampu, D.; Buruiana, E. C. Synthesis of Hybrid Nanocomposites Based on New Triazeno Copolymers and Montmorillonite Used for Detecting Metal Ions. *Polym. Int.* **2011**, *60*, 102−111.

(5) Sinha, J.; Kumar, A. Syntheses and Characterization of Amplified Fluorescence Poly(aryleneethynylene)s Based on 3,4-Propylenedioxythiophenes and Their Application in TNT Sensing. *Synth. Met.* **2010**, *160*, 2265−2272.

(6) Yang, J.-S.; Swager, T. M. Fluorescent Porous Polymer Films as TNT Chemosensors: Electronic and Structural Effects. *J. Am. Chem. Soc.* **1998**, *120*, 11864−11873.

(7) Rose, A.; Zhu, Z.; Madigan, C. F.; Swager, T. M.; Bulovic, V. Sensitivity Gains in Chemosensing by Lasing Action in Organic Polymers. *Nature* **2005**, *434*, 876−879.

(8) Liu, X.; Zhang, Q.; Xiong, Q.; Sum, T. C. Tailoring the Lasing Modes in Semiconductor Nanowire Cavities Using Intrinsic Self-Absorption. *Nano Lett.* **2013**, *13*, 1080−1085.

(9) Aad, R.; Blaize, S.; Bruyant, A.; Couteau, C.; Lérondel, G. Enhancement of Ultra-Thin Film Emission Using a Waveguiding Active Layer. *J. Appl. Phys.* **2010**, *108*, 123111−7.

(10) Yariv, A.; Yeh, P. *Photonics*, 6th ed.; Oxford University Press: New York, 2006.

(11) Le Barny, P.; Obert, E.; Soyer, F.; Malval, J. P.; Leray, I.; Lemaître, N.; Pansu, R.; Simic, V.; Doyle, H.; Redmond G.; Loiseaux, B. Detection of Nitroaromatic Compounds Based on Photoluminescent Side Chain Polymers. *SPIE Proc.* **2005**, vol. *5990*.

(12) Bojino, V.; Grabchev, I. A New Method for Synthesis of 4-Allyloxy-1,8-naphthalimide Derivatives for Use as Fluorescent Brighteners. *Dyes Pigm.* **2001**, *51*, 57−61.

(13) Ghorbanian, S.; Tyman, J.; Tychopoulos, V. J. The Synthesis of Symmetrical and Unsymmetrical Alkylaminonaphthalic-1,8-*N*-alkylimides. *Chem. Technol. Biotechnol.* **2000**, *75*, 1127−1134.

(14) Hamel, M.; Simic, V.; Normand, S. Fluorescent 1,8-Naphthalimides-Containing Polymers as Plastic Scintillators. An Attempt for Neutron−Gamma Discrimination. *React. Funct. Polym.* **2008**, *68*, 1671−1681.

(15) Tang, Z. K.; Wong, G. K. L.; Yu, P.; Kawasaki, M.; Ohtomo, A.; Koinuma, H.; Segawa, Y. Room-Temperature Ultraviolet Laser Emission from Self-Assembled ZnO Microcrystallite Thin Films. *Appl. Phys. Lett.* **1998**, *72*, 3270−3272.

(16) Tang, Z. K.; Kawasaki, M.; Ohtomo, A.; Koinuma, H.; Segawa, Y. Self-Assembled ZnO Nanocrystals and Exciton Lasing at Room Temperature. *J. Cryst. Growth* **2006**, *287*, 169−179.

(17) Zu, P.; Tang, Z. K.; Wong, G. K. L.; Kawasaki, M.; Ohtomo, A.; Koinuma, H.; Segawa, Y. Ultraviolet Spontaneous and Stimulated Emissions from ZnO Microcrystallite Thin Films at Room Temperature. *Solid State Commun.* **1997**, *103*, 459−463.

(18) Kawasaki, M.; Ohtomo, A.; Ohkubo, I.; Koinuma, H.; Tang, Z. K.; Yu, P.; Wong, G. K. L.; Zhang, B. P.; Segawa, Y. Excitonic Ultraviolet Laser Emission at Room Temperature from Naturally Made Cavity in ZnO Nanocrytal Thin Films. *Mater. Sci. Eng., B* **1998**, *56*, 239−244.

(19) Segawa, Y.; Ohtomo, A.; Kawasaki, M.; Koinuma, H.; Tang, Z. K.; Yu, P.; Wong, G. K. L. Growth of ZnO Thin Film by Laser MBE: Lasing of Exciton at Room Temperature. *Phys. Status Solidi B* **1997**, *202*, 669−672.

(20) Postava, K.; Sueki, H.; Aoyama, M.; Yamaguchi, T.; Ino, Ch.; Igasaki, Y.; Horie, M. Spectroscopic Ellipsometry of Epitaxial ZnO Layer on Sapphire Substrate. *J. Appl. Phys.* **2000**, *87*, 7820−7824.

(21) Yoshikawa, H.; Adachi, S. Optical Constants of ZnO. *Jpn. J. Appl. Phys.* **1997**, *36*, 6237−6243.

(22) Yu, P.; Tang, Z. K.; Wong, G. K. L.; Kawasaki, M.; Ohtomo, A.; Koinuma, H.; Segawa, Y. Room-Temperature Gain Spectra and Lasing in Microcrystalline ZnO Thin Films. *J. Cryst. Growth* **1998**, *184*, 601−605.

(23) Reynolds, D. C.; Look, D. C.; Jogai, B. Optically pumped ultraviolet lasing from ZnO. *Solid State Commun.* **1996**, *99*, 873−875.

(24) Bagnall, D. M.; Chen, Y. F.; Zhu, Z.; Yao, T.; Koyama, S.; Shen, M. Y.; Goto, T. Optically Pumped Lasing of ZnO at Room Temperature. *Appl. Phys. Lett.* **1997**, *70*, 2230−2232.

(25) Chen, Y.; Tuan, N. T.; Segawa, Y.; Ko, H.-J.; Hong, S.-K.; Yao, T. Stimulated Emission and Optical Gain in ZnO Epilayers Grown by

Plasma-Assisted Molecular-Beam Epitaxy with Buffers. *Appl. Phys. Lett.* **2001**, *78*, 1469−1471.
(26) Divay, L.; Rogers, D. J.; Lusson, A.; Kostcheev, S.; Mc Murtry, S.; Lérondel, G.; Hosseini Téhérani, F. Studies of Optical Emission in the High Intensity Pumping Regime of Top-down ZnO Nanostructures and Thin Films Grown on c-Sapphire Substrates by Pulsed Laser Deposition. *Phys. Status Solidi C* **2008**, *5*, 3095−3097.
(27) Cao, H.; Zhao, Y. G.; Ong, H. C.; Ho, S. T.; Dai, J. Y.; Wu, J. Y.; Chang, R. P. H. Ultraviolet Lasing in Resonators Formed by Scattering in Semiconductor Polycrystalline Films. *Appl. Phys. Lett.* **1998**, *73*, 3656−3658.
(28) Cao, H.; Zhao, Y. G.; Ho, S. T.; Seelig, E. W.; Wang, Q. H.; Chang, R. P. H. Random Laser Action in Semiconductor Powder. *Phys. Rev. Lett.* **1999**, *82*, 2278−2281.
(29) Dupont, P.-H.; Couteau, C.; Rogers, D. J.; Hosseini Téhérani, F.; Lérondel, G. Waveguiding-Assisted Random Lasing in Epitaxial ZnO Thin Film. *Appl. Phys. Lett.* **2010**, *97*, 261109−3.
(30) Svelto, O.; Hanna, D. C. *Principles of Lasers*, 4th ed.; Plenum Press: New York, 1998.
(31) Schroeder, R.; Ullrich, B. Absorption and Subsequent Emission Saturation of Two-Photon Excited Materials: Theory and Experiment. *Opt. Lett.* **2002**, *27*, 1285−1287.
(32) Coakley, K. M.; McGehee, M. D. Conjugated Polymer Photovoltaic Cells. *Chem. Mater.* **2004**, *16*, 4533−4542.
(33) Blumstengel, S.; Sadofev, S.; Puls, J.; Henneberger, F. An Inorganic/Organic Semiconductor "Sandwich" Structure Grown by Molecular Beam Epitaxy. *Adv. Mater.* **2009**, *21*, 4850−4853.
(34) Nguyen, H. M.; Seitz, O.; Aureau, D.; Sra, A.; Nijem, A.; Gartstein, Y. N.; Chabal, Y. J.; Malko, A. V. Spectroscopic Evidence for Nonradiative Energy Transfer between Colloidal CdSe/ZnS Nanocrystals and Functionalized Silicon Substrates. *Appl. Phys. Lett.* **2011**, *98*, 161904−3.
(35) Nimmo, M. T.; Caillard, L. M.; De Benedetti, W.; Nguyen, H. M.; Seitz, O.; Garstein, Y. N.; Chabal, Y. J.; Malko, A. V. Visible to Near-Infrared Sensitization of Silicon Substrates via Energy Transfer from Proximal Nanocrystals: Further Insights for Hybrid Photovoltaics. *ACS Nano* **2013**, *7*, 3236−3245.
(36) Aad, R.; Simic, V.; Le Cunff, L.; Rocha, L.; Sallet, V.; Sartel, C.; Lusson, A.; Couteau, C.; Lérondel, G. ZnO Nanowires As Effective Luminescent Sensing Materials for Nitroaromatic Derivatives. *Nanoscale* **2013**, *5*, 9176−9180.
(37) Benisty, H.; Stanley, R.; Mayer, M. Method of Source Terms for Dipole Emission Modification in Modes of Arbitrary Planar Structures. *J. Opt. Soc. Am. A* **1998**, *15*, 1192−1201.
(38) Duan, X.; Huang, Y.; Agarwal, R.; Lieber, C. M. Single-Nanowire Electrically Driven Lasers. *Nature* **2003**, *421*, 241−245.
(39) Chen, R.; Ling, B.; Sun, X. W.; Sun, H. D. Room Temperature Excitonic Whispering Gallery Mode Lasing from High-Quality Hexagonal ZnO Microdisks. *Adv. Mater.* **2011**, *23*, 2199−2204.